Comput. Methods Appl. Mech. Engrg. 272 (2014) 100–120

Contents lists available at ScienceDirect

Comput. Methods Appl. Mech. Engrg.

journal homepage: www.elsevier.com/locate/cma

Nonlocal vibrations of shell-type CNT conveying simultaneous internal and external flows by considering slip condition

Mehran Mirramezani, Hamid Reza Mirdamadi *, Mostafa Ghayour

Department of Mechanical Engineering, Isfahan University of Technology, 84156-83111 Isfahan, Iran

ARTICLE INFO

Article history:
Received 17 June 2013
Received in revised form 26 November 2013
Accepted 7 January 2014
Available online 13 January 2014

Keywords:
Fluid–structure interaction (FSI)
External flow
Divergence instability
Critical flow velocity
Slip condition
Nonlocal Donnell's shallow shell

ABSTRACT

In this article, the nonlocal but linear vibrations of carbon nano-tubular shells are analyzed subjected to both internal and external flows. This analysis is addressed for both separate flows as well as concurrent flows by considering slip condition. We observe that both nonlocal parameter and *Kn* could decrease the eigen-frequency and critical velocity of the first-mode divergence. It is observed that the existence of quiescent fluid does not impress the value of divergence velocity. Nonetheless, the frequencies are declined substantially. Besides, we perceive that CNT subjected to both internal and external flows loses its stability drastically sooner as compared with that subjected to each flow separately. Furthermore, it is observed that an increase in the value of mass density of the external flow results in a greater decrease in the eigen-frequencies as well as the divergence velocity.

© 2014 Elsevier B.V. All rights reserved.

1. Introduction

Carbon nano-tubes (CNTs) have exceptional mechanical, thermal, and electrical properties. Due to their perfect hollow cylindrical geometry and outstanding mechanical stiffness, CNTs are suitable for applications such as nano-containers and nano-pipes conveying fluid [1–4]. In this regard, several researchers studied the vibration characteristics of a beam-type CNT conveying fluid, such as natural frequency, stability, and critical mean flow velocity. Yoon et al. [5], Natsuki et al. [6], Lin and Qiao [7], Yan et al. [8], Ghavanloo et al. [9] and Wang et al. [10], made some of the key contributions in this area. Since a circular cylindrical shell structure develops shear forces, bending, and twisting moments to resist transverse loads by double curvatures, shell geometry is considerably stiffer than a corresponding beam. Consequently, different studies have been accomplished to analyze the stability of circular cylindrical shells conveying axial *internal* flows to obtain precise results [11–17]. Since cylindrical thin-walled structures simultaneously subjected to *internal* and *external* axial flows are common in engineering, different research groups endeavored to disclose the stability responses of beam and shell structures conveying *external* flow. Hannoyer and Païdoussis [18] studied theoretically and experimentally the dynamics of a pipe modeled as a beam with different boundary conditions, subjected to both interna1 and externa1 flows concurrently. They revealed that the stability status of a tubular beam subjected to both internal and external flows could not generally be inferred from the knowledge of its state when it was subjected to internal and external flows separately. However, if both internal and external flows were imposed simultaneously, the value of critical mean flow velocity was different. Selmane and Lakis [19] presented a general analysis for open cylindrical shells subjected to external and internal flows by neglecting free surface effects. They reported that the dynamical behavior of an open shell conveying both external and internal flows simultaneously was similar to those of complete circular cylindrical shells conveying fluid. The eigen-frequencies of each mode in

* Corresponding author. Tel.: +98 311 391 5248; fax: +98 311 391 2628.
E-mail addresses: m.mirramezani@me.iut.ac.ir (M. Mirramezani), hrmirdamadi@cc.iut.ac.ir (H.R. Mirdamadi), ghayour@cc.iut.ac.ir (M. Ghayour).

0045-7825/$ - see front matter © 2014 Elsevier B.V. All rights reserved.
http://dx.doi.org/10.1016/j.cma.2014.01.007

the absence of a dissipation mechanism decreased and eventually vanished with increasing the flow velocity. Amabili et al. [20] investigated the nonlinear dynamics of cylindrical shells in contact with axial external flowing fluid. They concluded that the dynamic response of a shell conveying external flow was quite quantitatively similar to that observed for internal flow.

Up to now, the effects of *external flow* on the stability response of shell-type CNTs conveying fluid has not been studied; however, in this article, we would attempt to fill this gap.

The major objective of the current research is to consider the size effects of nano-flow and nano-structure on the dynamic response of shell-type CNTs conveying non-viscous fluid. For studying the size effects imposed by a nano-structure, at present there are three major tools: experiments, molecular dynamic (MD) simulations, and continuum mechanics theories. Since the controlled and concise experiments on the vibrational behavior of CNTs conveying fluid are complicated and MD simulations involve formidable computational effort, the size-dependent continuum mechanical models seem to be more attractive to study the stability behaviors of beam and shell-type CNTs conveying fluid. Besides, the discrepancy between the predictions of continuum mechanics and the MD simulations could become smaller for CNTs with inner diameters larger than 6–10 fluid molecule diameters [21,22]. In recent years, several researchers have employed "partial" nonlocal elasticity theory of Eringen [23–26], "exact" nonlocal elasticity [27], modified couple stress [28], surface elasticity [29], and strain/inertia gradient elasticity theories [30] to realize the effects of length parameters on the vibrational characteristics of beam-type CNTs conveying fluid. The results from references [27–30] propose that an increase in the internal length scale parameter causes an increase in the critical mean flow velocities and eigen-frequencies, as opposed to the results obtained from "partial" nonlocal theory of Eringen.

In this study, we investigate the vibrational and stability behaviors of shell-type CNTs conveying fluid based on a linear nonlocal Donnell's shallow shell model. Chang and Lui [31] investigated the small scale effect on the flow-induced instability of double-walled carbon nano-tubes (DWCNTs) by using an elastic shell model based on Donnell's shell theory. They concluded that as the small scale effects were considered, the eigen-frequencies and the critical flow velocities of DWCNTs decreased as compared to the results from the classical local continuum mechanics. Jannesari et al. [32] analyzed the influence of nonlocal parameter on the structural stability of single-walled carbon nano-tubes (SWCNTs) modeled as a nonlinear Donnell's shallow shell. Their simulation results described destabilizing behavior of nonlocal effects, which attenuated by an increase in the tube radius from 3 to 9 nm. Moreover, they considered the effects of viscosity including a pressure drop and induced axial loads due to integration over viscosity shear stresses, and they inferred that viscosity had an enormous stabilizing effect. Ghorbanpour Arani et al. [33] studied the nonlinear vibration of DWCNT embedded in an elastic medium and subjected to an axial incompressible and non-viscous fluid flow. The small scale parameter, velocity, and fluid density were taken into account in their study to calculate the effects of axial and circumferential wave numbers. The results revealed that increasing circumferential wave number lead to added nonlinearity.

In the previously-mentioned studies [31–33], the size effects of *nano-flow* as well as the impression of simultaneous *external* and *internal* nano-flows were not addressed directly; however, in this research, we would pay more attention to these impressive effects. The effect of small-size in the study of fluid–structure interaction (FSI) problem for CNTs conveying *nano-flow* is not limited necessarily to the mechanical behavior of the structure part. Consequently, various research studies have been conducted to emphasize the significant role of size effects of *nano-flow* on the structural response of CNTs conveying fluid [34,35]. Rashidi et al. [34] developed an innovative FSI model for Euler–Bernoulli beam model conveying fluid by considering the slip boundary condition on the CNT walls. They proposed a dimensionless parameter velocity correction factor (*VCF*), i.e., the ratio of mean flow velocity by considering slip condition to the mean flow velocity with no-slip condition, and studied the effects of slip condition on the first-mode divergence stability. Mirramezani and Mirdamadi [35] investigated the role of *VCF* parameter on coupled-mode flutter instability of CNTs with different boundary conditions. The results of these studies [34,35] showed sooner occurrences for divergence and coupled-mode flutter instabilities by considering slip condition in comparison with those predicted by using continuum plug flow theory, i.e., $Kn = 0$. In some other studies, the effects of nano-size of both fluid flow and elastic structure were taken into account to discuss the stability response of nano-structures conveying nano-flow [36–38]. Kaviani and Mirdamadi [36] studied the wave propagation phenomena in beam-type CNT conveying fluid. The CNT structure was modeled by using size-dependent strain/inertia gradient theory of continuum mechanics and the CNT wall-fluid interaction by slip boundary condition and *Kn*. They reported that *Kn* could affect complex-valued wave frequencies at both lower and higher ranges of wave numbers, while the small-size had impression at the higher range. Mirramezani and Mirdamadi [37], and Matin et al. [38] analyzed the simultaneous size effects of nano-flow and nano-structure modeled as nano-beam and nano-plate, respectively, by considering *Kn* and nonlocal theory of Eringen. It was observed that, in a liquid nano-flow, most of the contribution in decreasing critical flow velocity was due to nonlocal parameter, but whenever the fluid was a gas, *Kn* could have a greater role in reducing the critical velocity. Moreover, the efficacy of the nonlocal parameter and *Kn* in the reduction of critical mean flow velocity seemed to be more remarkable for coupled-mode flutter [37,38]. Mirramezani et al. [39] reappraised the well-known equation of motion for a pipe conveying viscous fluid and concluded that the viscosity parameter of the fluid flow should not appear explicitly in the equation of motion of a pipe, modeled as a beam. Based on this result, they proposed a novel model for 1D coupled vibrations of CNTs conveying fluid using slip velocity of the fluid flow on the CNT walls as well as utilizing strain/inertia gradient theory and nonlocal continuum theory of Eringen to consider the size effects of both nano-flow and nano-structure. The results depicted that the critical mean flow velocity of the first-mode divergence instability obtained from this novel model was greater in comparison with the critical velocity predicted by the models using plug flow and classical continuum theories.

A thorough investigation of the literature reveals that the vibration and stability analysis of CNTs subjected to *internal* and *external flows* by considering the size effects of both *nano-flow* and *nano-shell* models has not been studied. In this article, we utilize a linear nonlocal Donnell's shallow shell model together with a linear fluid mechanics theory, that is, the potential flow theory for the incompressible and non-viscous fluid. By applying the nonlocal elasticity of Eringen to the classical Donnell's shell theory, we investigate the size-effect due to the flexible structure. Furthermore, we study the size effects of both internal and external flows by considering the slip condition on the CNT walls using *Kn*.

The remainder of this study is organized as follows. In Section 2, we derive the equation of motion of nonlocal Donnell's shallow shell conveying both internal and external flows. In Section 3, we implement the Galerkin's weighted residual solution techniques to solve the partial differential equations of nano-tube vibrations. In Section 4, we discuss stability analysis and present the results. Finally, in Section 5, we express our conclusions.

2. Model formulations

2.1. Linear Donnell's shallow shell theory

Fig. 1 shows a right circular cylindrical shell structure of the length L, radius R, and thickness h with the shell coordinate system x, θ, and z be the axial, circumferential, and radial coordinates of a nano-tube, respectively. Let u, v, and w be the corresponding displacement components of the shell; w is taken positive inward. Based on the Kirchhoff–Love's hypotheses, the displacement fields for time-dependent deformations are as follows [40]:

$$u(x,\theta,z,t) = u_0(x,\theta,t) - z\frac{\partial w_0}{\partial x} \tag{1}$$

$$v(x,\theta,z,t) = v_0(x,\theta,t) - \frac{z}{R}\frac{\partial w_0}{\partial \theta} \tag{2}$$

$$w(x,\theta,z,t) = w_0(x,\theta,t) \tag{3}$$

where u_0, v_0, and w_0 denote the displacements of a point on the mid-surface and t is the time. For linear small strains, the strain–displacement relations of a circular cylindrical shell take the form as follows [40]:

$$\varepsilon_{xx} = \varepsilon^0_{xx} + z\varepsilon^1_{xx} \tag{4}$$

$$\varepsilon_{\theta\theta} = \varepsilon^0_{\theta\theta} + z\varepsilon^1_{\theta\theta} \tag{5}$$

$$\gamma_{x\theta} = \gamma^0_{x\theta} + z\gamma^1_{x\theta} \tag{6}$$

where:

$$\varepsilon^0_{xx} = \frac{\partial u_0}{\partial x}, \quad \varepsilon^1_{xx} = -\frac{\partial^2 w_0}{\partial x^2} \tag{7}$$

$$\varepsilon^0_{\theta\theta} = \frac{1}{R}\frac{\partial v_0}{\partial \theta} - \frac{w_0}{R}, \quad \varepsilon^1_{\theta\theta} = -\frac{1}{R^2}\frac{\partial^2 w_0}{\partial \theta^2} \tag{8}$$

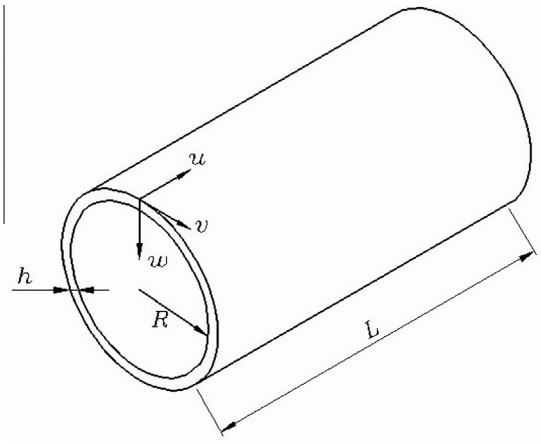

Fig. 1. Schematic diagram of a structural shell model of a CNT showing the coordinate system.

$$\gamma^0_{x\theta} = \frac{1}{R}\frac{\partial u_0}{\partial \theta} + \frac{\partial v_0}{\partial x}, \quad \gamma^1_{x\theta} = -\frac{2}{R}\frac{\partial^2 w_0}{\partial \theta \partial x} \tag{9}$$

The governing equations of motion of classical shell theory are derived using the extended Hamilton's principle. By considering the Kirchhoff–Love's hypotheses, i.e., $\varepsilon_{zz} = \gamma_{zx} = \gamma_{z\theta} = 0$, and neglecting the rotary inertia of the shell, the resultant external moments per unit area, and the components of external loads in the axial and circumferential directions, i.e., x and θ, the equilibrium equations are obtained as [40]:

$$\frac{\partial N_{xx}}{\partial x} + \frac{1}{R}\frac{\partial N_{x\theta}}{\partial \theta} = \rho_s h \frac{\partial^2 u_0}{\partial t^2} \tag{10}$$

$$\frac{\partial N_{x\theta}}{\partial x} + \frac{1}{R}\frac{\partial N_{\theta\theta}}{\partial \theta} = \rho_s h \frac{\partial^2 v_0}{\partial t^2} \tag{11}$$

$$\frac{\partial^2 M_{xx}}{\partial x^2} + \frac{2}{R}\frac{\partial^2 M_{x\theta}}{\partial x \partial \theta} + \frac{1}{R^2}\frac{\partial^2 M_{\theta\theta}}{\partial \theta^2} + \frac{N_{\theta\theta}}{R} + q_z = \rho_s h \frac{\partial^2 w_0}{\partial t^2} \tag{12}$$

where ρ_s is the mass density of the shell per unit volume of the shell and q_z is the lateral external load per unit area. It should be noticed that we obtain the essential and natural boundary conditions for an axially unconstrained, simply-supported cylindrical shell as $v_0 = w_0 = 0$, and $N_{xx} = M_{xx} = 0$ at $x = 0, L$, respectively. The stress resultants, which are forces per unit width, and the moment resultants, which are moments per unit length of circumferential direction are defined as:

$$N_{xx} = \int_{-h/2}^{h/2} \sigma_{xx} dz \quad N_{\theta\theta} = \int_{-h/2}^{h/2} \sigma_{\theta\theta} dz \quad N_{x\theta} = \int_{-h/2}^{h/2} \tau_{x\theta} dz \tag{13}$$

$$M_{xx} = \int_{-h/2}^{h/2} \sigma_{xx} z\, dz \quad M_{\theta\theta} = \int_{-h/2}^{h/2} \sigma_{\theta\theta} z\, dz \quad M_{x\theta} = \int_{-h/2}^{h/2} \tau_{x\theta} z\, dz \tag{14}$$

By applying the stress–strain and strain–displacement relations to calculate the stress and moment resultants and then substituting the resulting components into Eqs. (10)–(12), the equations of motion, i.e., Eqs. (10)–(12), could be expressed in terms of the displacements (u_0, v_0, w_0). Based on the assumption of Donnell's shell theory in which the in-plane inertias are neglected, i.e., $\ddot{u}_0$ and $\ddot{v}_0$ to be zero, the following system of coupled differential equations corresponding to the governing equations of motion of Donnell's shallow shell model are obtained [40]

$$\frac{\partial^2 u_0}{\partial x^2} + \frac{1-\nu}{2R^2}\frac{\partial^2 u_0}{\partial \theta^2} + \frac{1+\nu}{2R}\frac{\partial^2 v_0}{\partial \theta \partial x} - \frac{\nu}{R}\frac{\partial w_0}{\partial x} = 0 \tag{15}$$

$$\frac{1+\nu}{2R}\frac{\partial^2 u_0}{\partial \theta \partial x} + \frac{1-\nu}{2}\frac{\partial^2 v_0}{\partial x^2} + \frac{1}{R^2}\frac{\partial^2 v_0}{\partial \theta^2} - \frac{1}{R^2}\frac{\partial w_0}{\partial \theta} = 0 \tag{16}$$

$$-D\nabla^4 w_0 + \frac{Eh}{R(1-\nu^2)}\left(-\frac{w_0}{R} + \nu\frac{\partial u_0}{\partial x} + \frac{1}{R}\frac{\partial v_0}{\partial \theta}\right) + q_z = \rho_s h \frac{\partial^2 w_0}{\partial t^2} \tag{17}$$

where E is the Young's modulus, ν is the Poisson's ratio of the elastic shell and $D = Eh^3/12(1-\nu^2)$ is the bending rigidity of the shell and ∇^4 is a differential operator, as follows:

$$\nabla^4 = \frac{\partial^4}{\partial x^4} + \frac{2}{R^2}\frac{\partial^4}{\partial x^2 \partial \theta^2} + \frac{1}{R^4}\frac{\partial^4}{\partial \theta^4} \tag{18}$$

The coupling between in-plane displacements and lateral deflection could disappear for a linear Donnell's shallow shell theory and the uncoupled equation of motion is as follows [40]:

$$-D\nabla^8 w_0 - \frac{Eh}{R^2}\frac{\partial^4 w_0}{\partial x^4} = \nabla^4\left(\rho_s h \frac{\partial^2 w_0}{\partial t^2} - q_z\right) \tag{19}$$

where ∇^8 is a differential operator defined as:

$$\nabla^8 = \frac{\partial^8}{\partial x^8} + \frac{4}{R^2}\frac{\partial^8}{\partial x^6 \partial \theta^2} + \frac{6}{R^4}\frac{\partial^8}{\partial x^4 \partial \theta^4} + \frac{4}{R^6}\frac{\partial^8}{\partial x^2 \partial \theta^6} + \frac{1}{R^8}\frac{\partial^8}{\partial \theta^8} \tag{20}$$

The first term on the left hand side of Eq. (19) represents the flexural rigidity and the second term is the membrane rigidity due to the curvature of the Donnell's shallow shell. Eq. (19) is known as the uncoupled equation of motion for Donnell's shallow shell theory.

2.2. Nonlocal elastic Donnell's shell model

In the classical theory of elasticity, the stress tensor at the reference point x of a continuous body is exclusively a function of the local point strain tensor at x. Eringen [41] proposed the idea that for taking into account the small scale effects, the constitutive equations should be modified. The nonlocal stress tensor, denoted as $\sigma_{ij}^{n.l.}$ is computed from the local stress $\sigma_{ij}^{l.}$ tensor, indicated in the integral form as [41]:

$$\sigma_{ij}^{n.l.} = \int_V K(|x' - x|, \tau)\sigma_{ij}^{l.}(x')dx' \tag{21}$$

The kernel function $K(|x' - x|, \tau)$, represents the nonlocal weight function that is non-negative and decreasing for increasing distance values, $|x' - x|$ is the Euclidean distance and τ is the material constant that depends on internal and external characteristic lengths. Eq. (21) means that the nonlocal stress at a point x is a weighted average of the local stress of all points in the neighborhood of x. However, with the aim of making the elasticity equation simpler to solve, it is possible to represent an equivalent differential form as [42]:

$$(1 - (e_0a)^2\nabla^2)\sigma_{ij}^{n.l.} = C_{ijkl}\varepsilon_{kl} \tag{22}$$

where e_0 is a material constant, a is an internal characteristic length, ∇^2 is the Laplacian operator, which is equal to $\partial^2/\partial x^2 + \partial^2/R^2\partial\theta^2$, and C_{ijkl} denotes the fourth-order elasticity tensor. We apply the operator $(1 - (e_0a)^2\nabla^2)$ to Eqs. (15)–(17) to obtain the expressions for the nonlocal form of coupled differential equations of motion based on Donnell's shallow shell model as follows:

$$\frac{\partial^2 u_0}{\partial x^2} + \frac{1-\nu}{2R^2}\frac{\partial^2 u_0}{\partial \theta^2} + \frac{1+\nu}{2R}\frac{\partial^2 v_0}{\partial\theta\partial x} - \frac{\nu}{R}\frac{\partial w_0}{\partial x} = 0 \tag{23}$$

$$\frac{1+\nu}{2R}\frac{\partial^2 u_0}{\partial\theta\partial x} + \frac{1-\nu}{2}\frac{\partial^2 v_0}{\partial x^2} + \frac{1}{R^2}\frac{\partial^2 v_0}{\partial\theta^2} - \frac{1}{R^2}\frac{\partial w_0}{\partial\theta} = 0 \tag{24}$$

$$-D\nabla^4 w_0 + \frac{Eh}{R(1-\nu^2)}\left(-\frac{w_0}{R} + \nu\frac{\partial u_0}{\partial x} + \frac{1}{R}\frac{\partial v_0}{\partial\theta}\right) = \left\{(1 - (e_0a)^2\nabla^2)\left(\rho_s h\frac{\partial^2 w_0}{\partial t^2} - q_z\right)\right\} \tag{25}$$

It should be noticed that due to neglecting the in-plane inertias as well as the components of external loads in the axial and circumferential directions, the nonlocal and local forms of equations of motion in the axial and circumferential directions are similar. We can eliminate u and v from Eq. (25) by following the procedure of Ref. [40] to obtain an uncoupled equation of motion for nonlocal Donnell's shallow shell as follows:

$$-D\nabla^8 w_0 - \frac{Eh}{R^2}\frac{\partial^4 w_0}{\partial x^4} = (1 - (e_0a)^2\nabla^2)\nabla^4\left\{\rho_s h\frac{\partial^2 w_0}{\partial t^2} - q_z\right\} \tag{26}$$

2.3. Fluid–structure interaction for flowing fluid

The forces imposed by fluid on the shell are in terms of dynamic pressure and viscous shear stresses. The fluid–structure interaction (FSI) is described by the linear potential flow theory. The shell is considered to be conveying incompressible and non-viscous fluid. The fluid flow is assumed to be isentropic and irrotational. The irrotationality property is a condition for the existence of a scalar potential function ψ, from which the velocity vector $\vec{V}$ may be written as:

$$\vec{V} = \vec{\nabla}\psi \tag{27}$$

The velocity potential ψ is considered to be composed of a steady part due to the undisturbed mean flow velocity U in the axial direction, and another is an unsteady perturbed potential ϕ corresponding to the shell motions and vibrations. Consequently, the velocity potential function can be expressed as:

$$\psi = Ux + \phi \tag{28}$$

The components of the fluid velocity in the cylindrical coordinates (x, θ, r) are given by:

$$V_x = U + \frac{\partial\phi}{\partial x} \quad V_\theta = \frac{1}{r}\frac{\partial\phi}{\partial\theta} \quad V_r = \frac{\partial\phi}{\partial r} \tag{29}$$

It is assumed that the disturbances causing the deformations of the shell are sufficiently small for their squares and higher-order terms to be ignored. The continuity requires that the velocity field satisfies, $\nabla\cdot\vec{V} = 0$; this leads to the Laplace equation, $\nabla^2\psi = 0$, which may be expressed in terms of the potential of the disturbance, ϕ, as:

$$\frac{1}{r}\frac{\partial}{\partial r}\left(r\frac{\partial\phi}{\partial r}\right)+\frac{1}{r^2}\frac{\partial^2\phi}{\partial\theta^2}+\frac{\partial^2\phi}{\partial x^2}=0 \tag{30}$$

The boundary condition of impermeability of fluid-shell interface may be expressed mathematically as $Dw_0/Dt = V_r|_{r=R}$, where D/Dt is the material or total derivative. Thus, the condition is formulated as follows:

$$\left(\frac{\partial\phi}{\partial r}\right)_{r=R}=-\left(\frac{\partial w_0}{\partial t}+U\frac{\partial w_0}{\partial x}\right) \tag{31}$$

The perturbed pressure p may be related to the velocity potential by Bernoulli's equation for irrotational fluid flow, as follows:

$$\frac{\partial\phi}{\partial t}+\frac{V^2}{2}+\frac{p}{\rho_f}=0 \tag{32}$$

where ρ_f is the fluid mass density per unit volume, and $V^2 = V_x^2 + V_\theta^2 + V_r^2$. Hence, the perturbation pressure is found to be in terms of ϕ as follows:

$$p=-\rho_f\left(\frac{\partial\phi}{\partial t}+U\frac{\partial\phi}{\partial x}\right) \tag{33}$$

By using the method of separation of variables as well as assuming harmonic solution for vibrations of the simply-supported Donnell's shell in the lateral direction, the perturbation velocity potential becomes:

$$\phi(x,r,\theta,t)=\beta_{mn}(r)\sin\left(\frac{m\pi x}{L}\right)\cos(n\theta)W_{mn}(t) \tag{34}$$

where m is the axial half-wave number and n is the circumferential wave number. $W_{mn}(t)$ represents the generalized coordinates of the discretized system, and $\beta_{mn}(r)$ is a function to be determined later. By substituting Eq. (34) into Eq. (32), $\beta_{mn}(r)$ can be expressed as follows [43]:

$$\beta_{mn}(r)=C_0I_n\left(\frac{m\pi r}{L}\right)+C_1K_n\left(\frac{m\pi r}{L}\right) \tag{35}$$

where C_0 and C_1 are constant values and I_n and K_n are, respectively, the modified Bessel functions of the first and second kinds of order n. By using the condition that the velocity potential must be regular at $r = 0$, which means that $\beta_{mn}(r) = C_0I_n(m\pi r/L)$ for an *internal* flow and $\beta_{mn}(r) = C_1K_n(m\pi r/L)$ for an *external* flow, and satisfying Eq. (31), the potential ϕ may then be expressed as [43]:

Internal flow:

$$\phi_i(x,r,\theta,t)=-\frac{L}{m\pi}\frac{I_n(m\pi r/L)}{I_n'(m\pi R/L)}\left(\frac{\partial w_0}{\partial t}+U_i\frac{\partial w_0}{\partial x}\right) \tag{36}$$

External flow:

$$\phi_e(x,r,\theta,t)=-\frac{L}{m\pi}\frac{K_n(m\pi r/L)}{K_n'(m\pi R/L)}\left(\frac{\partial w_0}{\partial t}+U_e\frac{\partial w_0}{\partial x}\right) \tag{37}$$

where U_i and U_e are the undisturbed mean velocity of the internal and external flows, respectively. I_n' and K_n' are the first derivative of I_n and K_n, respectively. By substituting Eqs. (36) and (37) into Eq. (33), the perturbation pressure at the shell wall is found to be [43]:

Internal flow:

$$p_i=\rho_{if}\frac{L}{m\pi}\frac{I_n(m\pi r/L)}{I_n'(m\pi R/L)}\left(\frac{\partial}{\partial t}+U_i\frac{\partial}{\partial x}\right)^2 w_0 \tag{38}$$

External flow:

$$p_e=\rho_{ef}\frac{L}{m\pi}\frac{K_n(m\pi r/L)}{K_n'(m\pi R/L)}\left(\frac{\partial}{\partial t}+U_e\frac{\partial}{\partial x}\right)^2 w_0 \tag{39}$$

where ρ_{if} and ρ_{ef} are the internal and external fluid mass densities per unit volume, respectively. Therefore, the components of external loads per unit area exerted by the fluid flow on the CNT wall are expressed as:

$$q_z=-(p_i-p_e) \tag{40}$$

By substituting Eq. (40) into Eq. (26), we obtain an uncoupled equation of motion for Donnell's shallow shell conveying internal and external non-viscous fluid flows, as follows:

$$D\nabla^8 w_0 + \frac{Eh}{R^2}\frac{\partial^4 w_0}{\partial x^4} + (1-(e_0 a)^2\nabla^2)\nabla^4 \begin{pmatrix} \rho_s h \dfrac{\partial^2 w_0}{\partial t^2} + \rho_{if}\dfrac{L}{m\pi}\dfrac{I_n(m\pi r/L)}{I'_n(m\pi R/L)}\left(\dfrac{\partial}{\partial t}+U_i\dfrac{\partial}{\partial x}\right)^2 w_0 \\ -\rho_{ef}\dfrac{L}{m\pi}\dfrac{K_n(m\pi r/L)}{K'_n(m\pi R/L)}\left(\dfrac{\partial}{\partial t}+U_e\dfrac{\partial}{\partial x}\right)^2 w_0 \end{pmatrix} = 0 \tag{41}$$

2.4. Modeling slip boundary conditions

The study of nano-flow has attracted significant attentions in the recent years, since the fundamental issues encountered in nano-flow can be different from those of macro-flow because the surface to volume ratio is very high in nano-fluidic systems together with that the critical channel dimensions for a nano-flow can be comparable to the size of the fluid molecules under investigation. The mechanical behavior of a fluid depends on a variety of parameters and factors, in nano-size, probably the most influential is molecular mean free path. Some of the geometrical parameters could affect on the boundary conditions of fluid–structure interface, as well as fluid properties, like viscosity and mass density. One of the non-dimensional parameters is the Knudsen number (*Kn*). *Kn* is defined as the dimensionless ratio of the mean free path of the fluid molecules to a characteristic length of the flow geometry. According to *Kn*, four flow regimes may be identified: (1) $0 < Kn < 10^{-2}$, for the continuum flow regime, (2) $10^{-2} < Kn < 10^{-1}$, for the slip flow regime, (3) $10^{-1} < Kn < 10$, for the transition flow regime, and (4) $Kn > 10$, for the free molecular flow regime [44]. For CNTs conveying fluid, the *Kn* may be larger than 10^{-2}. Consequently, the flow regime is a slip flow. For slip flow regime, i.e., $10^{-2} < Kn < 10^{-1}$, the no-slip boundary condition theory fails, and a sub-layer, namely, Knudsen layer, should be a non-negligible part of the fluid flow from the wall surface. Thus, this phenomenon leads to a finite velocity slip, tangential to the wall surface. A formula for the effective viscosity of a fluid as a function of *Kn* in the slip regime is presented by Polard and Present [45], as follows:

$$\mu_e = \mu\left(\frac{1}{1+\alpha Kn}\right) \tag{42}$$

where μ_e is the effective viscosity, μ is the bulk viscosity, and α is a coefficient and could be calculated as follows [44]:

$$\alpha = \alpha_0\frac{2}{\pi}(\tan^{-1}(\alpha_1 Kn^B)) \tag{43}$$

The parameter values of $\alpha_1 = 4$, and $B = 0.4$ are obtained from experimental results. The coefficient α_0, can be obtained from the investigation of free molecular regime and is formulated as [44]:

$$\alpha_0 = \frac{64}{3\pi(1-\frac{4}{b})} \tag{44}$$

In Eq. (44), for a slip boundary condition of a second-order, b results to be -1. For considering the slip boundary condition into FSI equation of motion, we devise a velocity correction factor (*VCF*) concept for both internal and external flows. We multiply the undisturbed mean velocity of internal and external flows, i.e., U_i and U_e, along the axial direction by the dimensionless parameter *VCF*, which is defined as the ratio of the average flow velocity for a slip boundary condition to the average flow velocity for a corresponding no-slip boundary condition. The *VCF* for *internal flow* is defined as follows [35]:

$$VCF_{if} = (1+\alpha Kn)\left[1+4\left(\frac{2-\sigma_v}{\sigma_v}\right)\left(\frac{Kn}{1+Kn}\right)\right] \tag{45}$$

where σ_v is the tangential momentum accommodation coefficient and is considered to be 0.7 for most practical purposes [46]. In this research, we also consider the size-effect of *external nano-flow* on the stability response of CNT conveying fluid. Consequently, we present a *VCF* for *external flow* by following the same procedure as the reference [35]. To -provide the effect of slip boundary condition of the *external flow* on the FSI equation, we consider two parallel concentric shells with the same coordinate system as illustrated in Fig. 2. It should be noted that the inner tube is considered to be elastic and the outer tube is hypothesized to be a rigid structure. As a result, unsteady perturbed potential ϕ, might depend merely on the inner elastic shell motions and vibrations. Both internal and external flows are assumed to be homogeneous, laminar, fully developed, incompressible, isothermal, and irrotational. Beskok and Karniadakis [47] suggested Eq. (46) as a slip velocity model, which is claimed to be rather a more representative relation for correlating with the experimental data:

$$V_s - V_w = \left(\frac{2-\sigma_v}{\sigma_v}\right)\left(\frac{Kn}{1+Kn}\right)\left(\frac{\partial V_x}{\partial n}\right)_{r=R} \tag{46}$$

where V_s is the slip velocity of the fluid near the CNT wall surface, is the axial velocity of the solid wall as a rigid body, and n is an outward unit vector normal to the CNT wall surface. For simplicity of the following equations, we define a new parameter as:

$$\gamma \triangleq \left(\frac{2-\sigma_v}{\sigma_v}\right)\left(\frac{Kn}{1+Kn}\right) \tag{47}$$

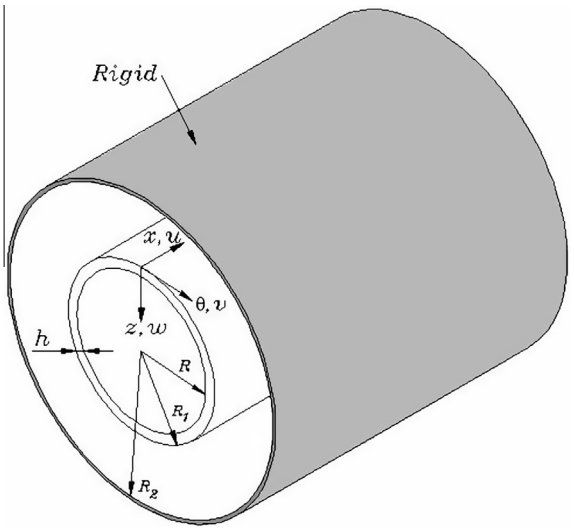

Fig. 2. Schematic diagram of an inner elastic tubular shell structure model of a CNT and its surrounding outer rigid shell.

The solution of the Navier–Stokes' equation in the axial direction of an orthogonal cylindrical coordinate system for a pipe with the inner radius R_1 and outer radius R_2, is as follows [48]:

$$V_x = \frac{1}{4\mu}\left(\frac{\partial p}{\partial x}\right) r^2 + D_0 ln(r) + D_1 \tag{48}$$

where D_0 and D_1 are integration constants. For *internal flow*, the condition that the velocity potential must be regular at $r = 0$, enforces $D_0 = 0$; however, for *external flow*, none of the integration constants could be equal to zero. D_0 and D_1 are obtained by considering boundary conditions for slip condition as:

$$\begin{cases} r = R_1 \rightarrow V_x = V_{s1} \\ r = R_2 \rightarrow V_x = V_{s2} \end{cases} \tag{49}$$

where V_{s1} and V_{s2} are the slip velocities on the outer surface of the inner tube and inner surface of the outer tube, respectively. By substituting Eq. (49) into Eq. (48), we have:

$$\begin{cases} V_{s1} = \frac{1}{4\mu}\left(\frac{\partial p}{\partial x}\right) R_1^2 + D_0 ln(R_1) + D_1 \\ V_{s2} = \frac{1}{4\mu}\left(\frac{\partial p}{\partial x}\right) R_2^2 + D_0 ln(R_2) + D_1 \end{cases} \tag{50}$$

In another way, we consider $V_w = 0$ and replacing $(\partial V_x/\partial n)_{r=R_1}$ by $R_1(\partial V_x/\partial r)_{r=R_1}$ and $(\partial V_x/\partial n)_{r=R_2}$ by $-R_2(\partial V_x/\partial r)_{r=R_2}$ in Eq. (46), and computing $\partial V_x/\partial r$ from Eq. (48), we could rewrite the slip velocity at the CNT wall as:

$$\begin{cases} V_{s1} = \gamma R_1 \left(\frac{1}{2\mu}\frac{\partial p}{\partial x} R_1 + \frac{D_0}{R_1}\right) \\ V_{s2} = -\gamma R_2 \left(\frac{1}{2\mu}\frac{\partial p}{\partial x} R_2 + \frac{D_0}{R_2}\right) \end{cases} \tag{51}$$

By substituting the terms for V_{s1} and V_{s2} from Eq. (51) into the left hand sides of Eq. (50), we could obtain the integration constants D_0 and D_1. It should be noted that the expressions for these constants are given in Appendix A. Due to a tendency for defining the *VCF* for *external flow* with the same procedure as utilized by Mirramezani and Mirdamadi [35], we need to calculate only the mean flow velocity by considering slip condition. Therefore, if we consider the slip velocity at the wall of nano-tube for calculating the constants D_0 and D_1 in Eq. (48) and integrate Eq. (48) over the cross sectional area of the pipe, the average flow velocity is as follows:

$$\bar{V}_{slip} = \frac{1}{8\mu}\left(\frac{\partial p}{\partial x}\right)(R_1^2 + R_2^2) + \frac{D_0}{(R_2^2 - R_1^2)}\left(R_2^2\left(\ln R_2 - \frac{1}{2}\right) - R_1^2\left(\ln R_1 - \frac{1}{2}\right)\right) + D_1 \tag{52}$$

As we observe from Appendix A, D_0 and D_1 are functions of γ that depends on *Kn*. We represent the ratio of the mean *external flow* velocity through the tube, incorporating slip condition, to the mean flow velocity through the pipe, considering no-slip condition, as follows:

$$VCF_{ef} = \frac{\bar{V}_{slip}}{\bar{V}_{no\text{-}slip}} \tag{53}$$

It should be noticed that $\bar{V}_{slip}$ is a function of Kn and could be calculated by Eq. (52), while $\bar{V}_{no-slip}$ could be derived by setting Kn to zero in Eq. (52), i.e., $\bar{V}_{slip}$. For considering the slip boundary condition into FSI equation of motion, we multiply the undisturbed mean flow velocities U_i and U_e along the axial direction by the dimensionless parameters VCF_{if} and VCF_{ef}, respectively. Therefore, the FSI equations of motion for nonlocal Donnell's shell conveying both *internal and external flows* by considering the slip conditions are obtained as:

$$D\nabla^8 w_0 + \frac{Eh}{R^2}\frac{\partial^4 w_0}{\partial x^4} + (1-(e_0a)^2\nabla^2)\nabla^4 \begin{pmatrix} \rho_s h \dfrac{\partial^2 w_0}{\partial t^2} + \rho_{if}\dfrac{L}{m\pi}\dfrac{I_n(m\pi R/L)}{I'_n(m\pi R/L)}\left(\dfrac{\partial}{\partial t} + VCF_{if}U_i\dfrac{\partial}{\partial x}\right)^2 w_0 \\ -\rho_{ef}\dfrac{L}{m\pi}\dfrac{K_n(m\pi R/L)}{K'_n(m\pi R/L)}\left(\dfrac{\partial}{\partial t} + VCF_{ef}U_e\dfrac{\partial}{\partial x}\right)^2 w_0 \end{pmatrix} = 0 \tag{54}$$

where I_n, I'_n, K_n, and K'_n were defined at Eqs. (35)–(37). Eq. (54) is rendered dimensionless through the use of dimensionless parameters as:

$$(a)\ \eta = \frac{w_0}{L}, \quad (b)\ \xi = \frac{x}{L}, \quad (c)\ \tau = \left(\frac{D}{\rho_s h}\right)^{\frac{1}{2}}\frac{\pi^2}{L^2}t, \quad (d)\ \hat{H} = \frac{L}{h}, \quad (e)\ \hat{R} = \frac{L}{R} \tag{55}$$

$$(f)\ u_i = \left(\frac{\rho_s h}{D}\right)^{\frac{1}{2}}\frac{L}{\pi^2}U_i \quad (g)\ u_e = \left(\frac{\rho_s h}{D}\right)^{\frac{1}{2}}\frac{L}{\pi^2}U_e \quad (h)\ \lambda = \frac{Eh}{D}\frac{L^4}{R^2} \quad (i)\ \bar{\lambda} = 12(1-\nu^2)\hat{H}^2\hat{R}^2$$

$$(j)\ \mu = \frac{e_0a}{L} \quad (k)\bar{\mu} = \frac{e_0a}{R} \quad (l)\ \beta_i = \pi^4\frac{\rho_{if}}{\rho_s}\frac{I_n(m\pi R/L)}{I'_n(m\pi R/L)} \quad (m)\ \beta_e = \pi^4\frac{\rho_{ef}}{\rho_s}\frac{K_n(m\pi R/L)}{K'_n(m\pi R/L)}$$

Finally, the dimensionless governing equation by considering the nonlocal theory of Eringen and slip condition is as follows:

$$\bar{\nabla}^8\eta + \lambda\frac{\partial^4\eta}{\partial\xi^4} + (1-\mu^2\frac{\partial^2}{\partial\xi^2} - \bar{\mu}^2\frac{\partial^2}{\partial\theta^2})\bar{\nabla}^4 \begin{pmatrix} \pi^4\dfrac{\partial^2\eta}{\partial\tau^2} + \dfrac{\beta_i}{m\pi}\hat{H}\left(\dfrac{\partial^2\eta}{\partial\tau^2} + 2(VCF_{if})u_i\dfrac{\partial^2\eta}{\partial\xi\partial\tau} + (VCF_{if})^2u_i^2\dfrac{\partial^2\eta}{\partial\xi^2}\right) \\ -\dfrac{\beta_e}{m\pi}\hat{H}\left(\dfrac{\partial^2\eta}{\partial\tau^2} + 2(VCF_{ef})u_e\dfrac{\partial^2\eta}{\partial\xi\partial\tau} + (VCF_{ef})^2u_e^2\dfrac{\partial^2\eta}{\partial\xi^2}\right) \end{pmatrix} = 0 \tag{56}$$

where $\bar{\nabla}^4$ and $\bar{\nabla}^8$ are presented in Eqs. (57) and (58) as follows:

$$\bar{\nabla}^4 = \frac{\partial^4}{\partial\xi^4} + 2\hat{R}^2\frac{\partial^4}{\partial\xi^2\partial\theta^2} + \hat{R}^4\frac{\partial^4}{\partial\theta^4} \tag{57}$$

and

$$\bar{\nabla}^8 = \frac{\partial^8}{\partial\xi^8} + 4\hat{R}^2\frac{\partial^8}{\partial\xi^6\partial\theta^2} + 6\hat{R}^4\frac{\partial^8}{\partial\xi^4\partial\theta^4} + 4\hat{R}^6\frac{\partial^8}{\partial\xi^2\partial\theta^6} + \hat{R}^8\frac{\partial^8}{\partial\theta^8} \tag{58}$$

It should be noted that Eh and D for CNTs are obtained experimentally and we define a dimensionless parameter λ for shell-type CNT conveying fluid. However, as far as D is considered as $D = Eh^3/12(1-\nu^2)$, in general, the dimensionless parameter $\bar{\lambda}$ is a more appropriate parameter.

3. Solution method

In order to solve the uncoupled equation of motion for nonlocal Donnell's shallow shell subjected to simultaneous *internal and external fluid flows* by considering the slip condition and study the divergence instability condition, we use Galerkin's approximate solution method. In our study, a simply-supported circular cylindrical shell conveying fluid is considered. Hence, the lateral displacement w_0 of the shell can be expanded to satisfy the essential and natural boundary conditions; i.e., w_0 and M_{xx} are equal to zero at $x = 0, L$, by assuming the following form:

the lateral deflection:

$$w_0(x,\theta,t) = \sin\left(\frac{m\pi x}{L}\right)\cos(n\theta)W_{mn}(t) \tag{59}$$

or equivalently the dimensionless lateral deflection:

$$\eta(\xi,\theta,\tau) = \sin(m\pi\xi)\cos(n\theta)\Psi_{mn}(\tau) \tag{60}$$

where m and n are the number of longitudinal half-waves, and the number of circumferential waves, respectively. In Eq. (64), $\sin(m\pi x/L)\cos(n\theta)$ is the comparison function, i.e., the (m,n)th eigen-function of a shell with the same boundary conditions but no consideration of interaction between the fluid and structure; and $W_{mn}(t)$ represents the generalized coordinates of the discretized system corresponding to the mode (m,n) and is expressed as follows:

$$W_{mn}(t) = Q_{mn}e^{st} \tag{61}$$

where Q_{mn} is the constant amplitude of generalized coordinate of CNT free vibrations and s denotes the complex-valued eigen-frequency corresponding to this mode.

3.1. Discretization

In this subsection, we use Galerkin's weighted-residual technique for simply-supported shell, using the derived uncoupled equation of motion, i.e. Eqs. (54) and (55). In this approximate method, we use the strong form of governing differential equations of motion to compute the residual. For this purpose, we start discretizing by choosing one generalized coordinate. We substitute the approximate function of Eqs. (59) and (60) into the fundamental differential Eq. (54) or Eq. (56) to calculate the residual. Then, we multiply this residual by a weight function, i.e., test function. Herein, the comparison and the weight functions are the same and are selected as the first mode eigen-function, i.e., either $\sin(m\pi x/L)\cos(n\theta)$, or $\sin(m\pi\xi)\cos(n\theta)$ for the dimensionless form. The resulting weighted residual is then integrated over the domain of the structure. This integrated weighted residual is then set to zero, for satisfying the orthogonality principle of error to information space. The coefficients of $W_{mn}(t)$, and $\ddot{W}_{mn}(t)$ are denoting the equivalent stiffness (K_{eq}), and mass (M_{eq}) parameters of the discretized system as a SDOF, respectively. If we define $\psi = m\pi/L$ and $\bar{\psi} = m\pi$, the equivalent mass and stiffness parameters of a nonlocal simply-supported Donnell's shell conveying both *internal and external fluid* corresponding to Eq. (54) or Eq. (56) become, as follows:

the equivalent mass parameter:

$$M_{eq} = \left(1 + (e_0a)^2\left[\psi^2 + \left(\frac{n}{R}\right)^2\right]\right)\left(\psi^4 + 2\left(\frac{n}{R}\right)^2\psi^2 + \left(\frac{n}{R}\right)^4\right)\left(\rho_s h + \frac{\rho_{if}}{\psi}\frac{I_n(m\pi R/L)}{I'_n(m\pi R/L)} - \frac{\rho_{ef}}{\psi}\frac{K_n(m\pi R/L)}{K'_n(m\pi R/L)}\right) \tag{62}$$

or equivalently the dimensionless equivalent mass parameter:

$$\bar{M}_{eq} = (1 + (\mu\bar{\psi})^2 + (\bar{\mu}n)^2)(\bar{\psi}^4 + 2n^2\hat{R}^2\bar{\psi}^2 + n^4\hat{R}^4)\left(\pi^4 + \frac{\beta_i}{\bar{\psi}}\hat{H} - \frac{\beta_e}{\bar{\psi}}\hat{H}\right) \tag{63}$$

the equivalent stiffness parameter:

$$\begin{aligned} K_{eq} = {} & D\left(\psi^8 + 4\left(\frac{n}{R}\right)^2\psi^6 + 6\left(\frac{n}{R}\right)^4\psi^4 + 4\left(\frac{n}{R}\right)^6\psi^2 + \left(\frac{n}{R}\right)^8\right) + \frac{Eh}{R^2}\psi^4 \\ & - \left(1 + (e_0a)^2\left[\psi^2 + \left(\frac{n}{R}\right)^2\right]\right)\left(\psi^6 + 2\left(\frac{n}{R}\right)^2\psi^4 + \left(\frac{n}{R}\right)^4\psi^2\right)\left(\frac{\rho_{if}}{\psi}\frac{I_n(m\pi R/L)}{I'_n(m\pi R/L)}(VCF_{if})^2U_i^2 - \frac{\rho_{ef}}{\psi}\frac{K_n(m\pi R/L)}{K'_n(m\pi R/L)}(VCF_{ef})^2U_e^2\right) \end{aligned} \tag{64}$$

or equivalently the dimensionless equivalent stiffness parameter:

$$\begin{aligned} \bar{K}_{eq} = {} & (\bar{\psi}^8 + 4n^2\hat{R}^2\bar{\psi}^6 + 6n^4\hat{R}^4\bar{\psi}^4 + 4n^6\hat{R}^6\bar{\psi}^2 + n^8\hat{R}^8) + \lambda\bar{\psi}^4 - (1 + (\mu\bar{\psi})^2 + (\bar{\mu}n)^2)(\bar{\psi}^6 + 2n^2\hat{R}^2\bar{\psi}^4 + n^4\hat{R}^4\bar{\psi}^2) \\ & \times \left(\frac{\beta_i}{\bar{\psi}}\hat{H}(VCF_{if})^2u_i^2 - \frac{\beta_e}{\bar{\psi}}\hat{H}(VCF_{ef})^2u_e^2\right) \end{aligned} \tag{65}$$

Eqs. (64) and (65) are denoting the elastic stiffness parameter due to in-plane and bending rigidities of the shell as well as a geometric stiffness parameter owing to the centripetal acceleration effects.

4. Results and discussion

In this section, we utilize the approximate solution of Galerkin for simulating numerically the behavior of fluid passing through the nano-pipe. Following most published papers on CNTs, the wall thickness of CNTs under consideration is taken as 0.34 nm, i.e. $h = 0.34$ nm, and the mass density of the CNT is $\rho_{CNT} = 2.3\ \mathrm{g\ cm^{-3}}$ [51]. We may consider other material and geometrical properties of nano-tube as follows: inner radius $R = 100h$; CNT length $L = 2R$; mass density of acetone $\rho_{ace} = 0.79\ \mathrm{g\ cm^{-3}}$, the mass density of air $\rho_{air} = 0.001169\ \mathrm{g\ cm^{-3}}$, the mass density of water $\rho_{air} = 1\ \mathrm{g\ cm^{-3}}$ and the mass density of ether $\rho_{eth} = 0.079\ \mathrm{g\ cm^{-3}}$.

4.1. Validation

In this subsection, we would like to compare our numerical results, obtained by Galerkin's method, with those of Amabili [50]. Since Amabili [50] investigates a simply-supported circular cylindrical local Donnell's shell conveying internal

non-viscous water flow by considering no-slip condition, we need to substitute the ρ_{ef} and nonlocal parameters in Eq. (54) to zero in addition that we are enforced to choose the internal and external velocity correction factors equal to one. We consider the material and geometrical characteristics as follows [50]: $L/R = 2$, $h/R = 0.01$, $E = 206 \times 10^9$ N m^{-2}, $\rho_s = 7850$ kg m^{-3}, $\rho_f = 1000$ kg m^{-3}, and $v = 0.3$. Fig. 3 shows how the imaginary parts of the first two eigen-frequencies change for the various values of mean flow velocity of the water, i.e., u_i, through a simply-supported linear Donnell's shallow shell for modes having five circumferential waves and including the longitudinal fundamental mode, i.e., $n = 5$ and $m = 1$. As the mean flow velocity increases from zero to a critical value, these frequencies approach zero, showing the deterioration of the pipe bending stiffness. For critical flow velocities, the resonant frequencies become zero, and the divergence or static instability occurs. As we could observe from Fig. 3 the first buckled equilibrium solution, i.e., the first-mode divergence instability arises at $u_i = 3.335$ and the second-mode divergence instability could occur at $u_i = 4.336$, as we could have expected from the observations of Amabili [50]. Since our results seem to be in good agreement with those of reference [50], we could rely on our numerical algorithm to continue the analysis of the dynamic stability of CNTs conveying fluid based on the properties given at Section 4.

4.2. Effects of external flow on stability analysis

One of the debatable subjects in the current research is studying the stability of shell-type CNTs conveying fluid flows of internal and external, flowing either simultaneously or separately. Consequently, in this subsection, we analyze the stability response of Donnell's shell structure subjected to external flow and compare with that of internal flow. Moreover, we pay special attention to the impression of concurrent flows on the first-mode divergence stability of shell-type CNTs. According to Païdoussis [49], if the equivalent stiffness of a system becomes zero for some critical value of the fluid flow velocity, then the overall stiffness of the system vanishes, which signifies that the divergence instability occurs. If we consider K_{eq} and $\bar{K}_{eq}$ equal to zero, then we could calculate the critical divergence velocity by considering nonlocal elasticity for shell-type CNT conveying both *internal and external* nano-flows. If we neglect the nano-size effects on the nano-flow, i.e., *VCF*, as well as on the nano-shell, i.e., nonlocal parameter, and set the $\bar{K}_{eq}$ to zero, we are able to contrast critical mean *external* against *internal* flow velocity. We consider the material and geometrical characteristics, as follows, [50]: $L/R = 2$, $h/R = 0.01$, $E = 206 \times 10^9$ N m^{-2}, $\rho_s = 7850$ kg m^{-3}, $\rho_{if} = \rho_{ef} = 1000$ kg m^{-3}, $v = 0.3$, $n = 5$, and $m = 1$.

Fig. 4 illustrates how the variations in the critical mean velocities of internal and external flows are interrelated. In this section, both internal and external flows along the shell structure are considered to be water. Whenever the mean velocity for external flow is assumed to be zero in Eq. (65), this is equivalent to saying that the external flow should be quiescent. It should be noted that in the following parts of this paper, we make clear that the presence of quiescent fluid could not change the critical velocity of the first-mode divergence. For this case, the first-mode divergence dimensionless critical flow velocity is obtained to be 3.336, which is quite in accordance with the results from Amabili [50], where only internal flow is considered. On the contrary, if the mean velocity for internal flow were considered zero in Eq. (65), meaning to have both internal quiescent fluid and the vibration of the shell structure subjected to only external flow, the critical mean velocity of the first-mode divergence for the shell under the external flow becomes very close to the previous case, i.e., 3.364. This closeness of results could be due to using the same density for both external and internal flows. In addition, regarding the wave numbers with values $m = 1$ and $n = 5$, and $L = 2R$, the expressions I_n/I'_n and K_n/K'_n have very close numerical values. From Fig. 4, we may observe that if the nano-shell could be subjected to an external flow with a given mean velocity, the mean velocity

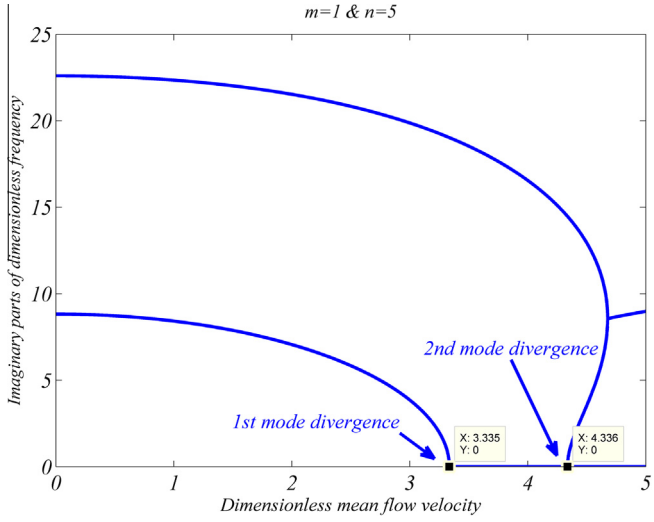

Fig. 3. Imaginary parts of the first two non-dimensional eigen-frequencies of a simply-supported Donnell's shallow shell with $n = 5$ and $m = 1$ against dimensionless mean flow velocity for water.

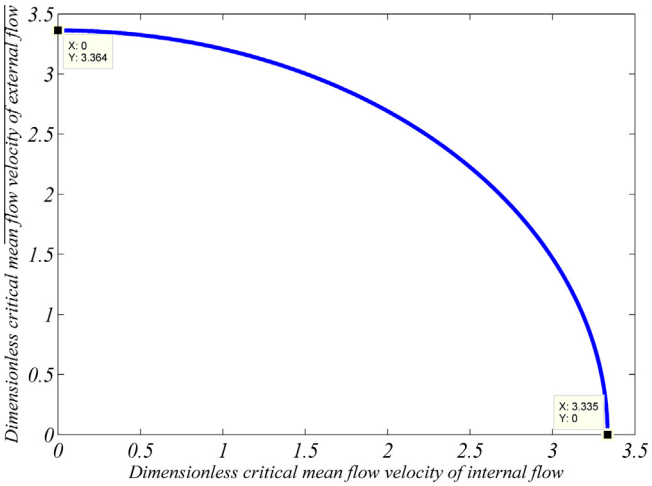

Fig. 4. Dimensionless critical mean velocity of an external flow (water) against dimensionless critical mean velocity of an internal flow (water) of a macro-scale simply-supported Donnell's shallow shell with $n = 5$ and $m = 1$.

of the corresponding internal flow changes such that with a given rise in the mean velocity of external flow, the first-mode divergence critical mean velocity of the internal flow decreases. The same phenomenon could be observed by switching between internal and external flows.

In general, setting Eq. (65) to zero and regarding u_i and u_e as variables, we reach the equation of an ellipse, since the values of modified Bessel functions of the first and second kinds are always positive as well as the first derivative of the modified Bessel functions of the first kind. However, the reverse is true for the first derivative of the modified Bessel function of the second kind; hence, the coefficients of u_i^2 and u_e^2 are always positive. Moreover, if the fluid density of the internal and external flows were different, even the closeness of the values of I_n/I'_n and K_n/K'_n could not cause that the critical velocities of either internal or external flow would become the same or even close to each other. Rather it becomes different depending on the type of problem at hand.

Fig. 5 indicates the imaginary parts of the complex-valued eigen-frequencies of a Donnell's shallow shell against the average velocity of the liquid (acetone) flow. By comparing the fundamental frequencies as well as the critical mean flow velocity of CNT conveying either internal or external flows, we observe an insignificant increase in the value of eigen-frequencies and critical velocities for the external flow in contrast to internal flow. As a result, we conclude that the dynamical behavior of a simply-supported Donnell's shell conveying external flow is quite similar qualitatively to that obtained for internal flow. Fig. 6 depicts the dynamic response of CNTs subjected concurrently to both internal and external liquid flow. The results

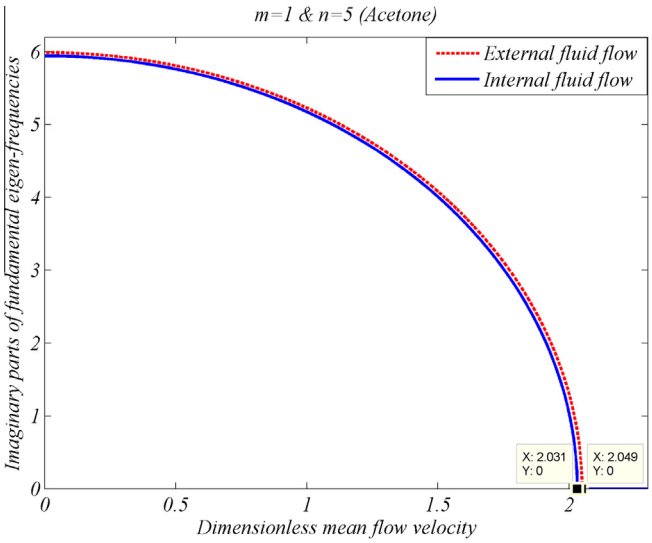

Fig. 5. Imaginary parts of the fundamental eigen-frequencies of simply-supported Donnell's shallow shell against dimensionless mean flow velocity for both internal and external flows of acetone.

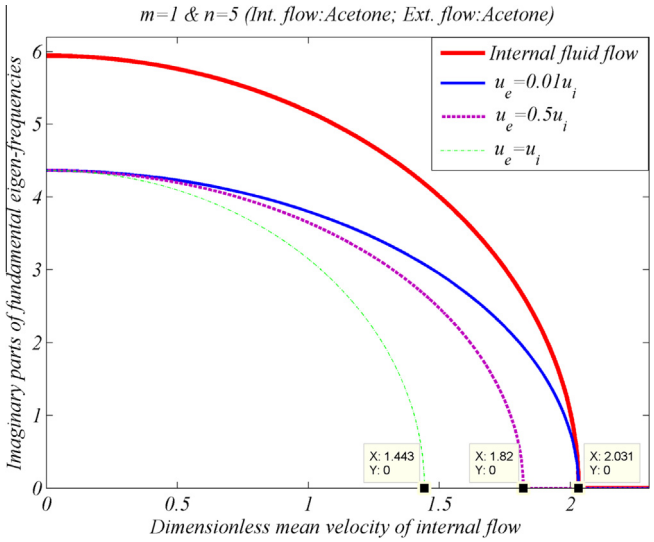

Fig. 6. Imaginary parts of the fundamental eigen-frequencies of simply-supported Donnell's shallow shell conveying simultaneous internal and external flows of acetone against dimensionless mean flow velocity for an internal flow of acetone considering different values of u_e/u_i.

of this figure are obtained by considering a constant ratio for the mean velocity of the external flow to that of internal flow. We notice that if we consider a very slow mean velocity for external flow, herein: $u_e = 0.01u_i$, the external flow effects on the stability, i.e., the eigen-frequency and critical velocity, are very identical to that of an external quiescent fluid. As we choose a higher value for the average velocity of external flow, we perceive that the first-mode divergence instability could occur drastically sooner. Fig. 7 illustrates the dependency of critical mean velocity of internal flow on the external mean flow velocity and vice versa, for acetone as an internal flow. As could be seen, by choosing a fixed value for the average velocity of external flow, the critical internal flow velocity of the first-mode divergence could decrease. Therefore, the presence of either external or internal flow alters the divergence velocity of the corresponding internal or external flow, respectively. Besides, it could be inferred from Fig. 7 that as the external fluid could have greater mass density, the efficacy of the external flow for a reduction in the critical velocity should be more substantial. For instance, regarding a fixed value for both acetone and water external flows equal to 1.5, the critical values for internal acetone flow become 1.383 and 1.151 for shell-type CNT subjected to acetone and as water external flows, respectively. Therefore, a water external flow in comparison with an acetone external flow reduces the critical velocity for the internal flow more severely, because the water fluid is denser than the acetone.

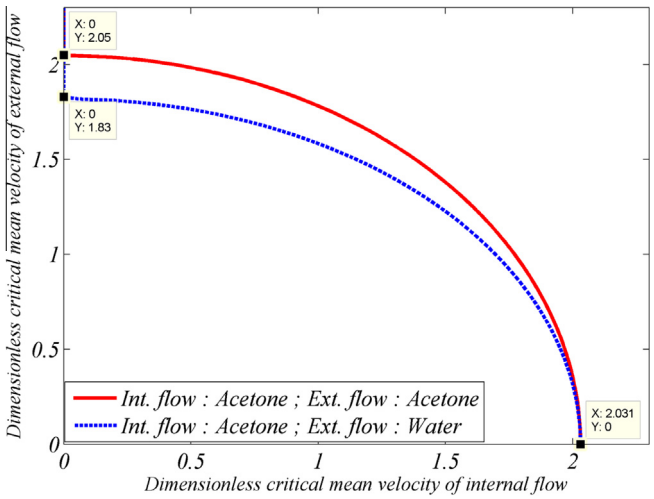

Fig. 7. Dimensionless critical mean flow velocity of external flows of water and acetone against dimensionless critical mean flow velocity of an internal flow of acetone for a simply-supported Donnell's shallow shell-type CNT with $n = 5$ and $m = 1$.

4.3. Effect of quiescent fluid on the first-mode divergence

In this subsection, we consider free vibrations of linear local circular cylindrical Donnell's shell with simply-supported ends, completely filled with a quiescent and *incompressible* fluid. It is worth mentioning that for studying the influence of a quiescent external fluid on the critical mean flow velocity and eigen-frequency of the Donnell's shell conveying an internal flow, we consider U_e in Eq. (54) equal to zero. Consequently, we investigate the effect of a virtual density factor, i.e., ρ_v, as added to the mass density of the shell-type CNT for either internal or external *incompressible* fluids, as follows:

a virtual density factor as added to an internal flow with a quiescent external fluid:

$$\rho_v = -\rho_{ef}\frac{L}{m\pi}\frac{K_n(m\pi R/L)}{K_n'(m\pi R/L)} \tag{66}$$

a virtual density factor as added to an external flow with a quiescent internal fluid:

$$\rho_v = \rho_{if}\frac{L}{m\pi}\frac{I_n(m\pi R/L)}{I_n'(m\pi R/L)} \tag{67}$$

It should be noticed that both ρ_vs obtained from Eqs. (66) and (67) are positive-valued, because $-K_n/K_n'$ and I_n/I_n' are always greater than zero. Figs. 8 and 9 demonstrate the imaginary parts of fundamental eigen-frequencies versus the mean flow velocity for a simply-supported Donnell's shell with $n = 5$ and $m = 1$, conveying an internal fluid flow, i.e., acetone, with a quiescent external fluid, i.e., acetone, and vice versa, respectively. As we observe from these two figures, the presence of a quiescent fluid could not change the value of critical mean flow velocity. However, as expected, a remarkable decrement of eigen-frequencies is perceived. The decrease in the eigen-frequencies is due to increase in the equivalent mass parameter of the discretized system by considering the virtual added density.

4.4. Effect of nonlocal elasticity on the first-mode divergence

In this subsection, we investigate the effect of nonlocal parameter on the dynamic stability of a nano-shell conveying fluid in a continuum flow regime, i.e., $Kn = 0$. Since, the stability responses of Donnell's shell subjected to both internal and external flows are quite analogous, in this part, we analyze the impact of nonlocality on just the internal flow without the presence of a quiescent or moving external fluid. It should be noticed that a large range of values for the size-effect coefficient of e_0a is possible; however, in the present study, we consider e_0a between zero and 2 nm, according to Wang et al. [52]. Since the nonlocal elasticity theory is used to consider the size effect of an elastic structure, herein a CNT, the range of nonlocal parameter is independent of the liquid and gas nano-flows. Consequently, in this subsection, we discuss the effect of nonlocal parameter, i.e., e_0a, on the first-mode divergence instability of CNTs conveying liquid. Fig. 10 illustrates the imaginary parts of the fundamental eigen-frequencies versus the mean flow velocity for a simply-supported Donnell's shell with $n = 5$ and $m = 1$, conveying acetone by considering two values of e_0a. As we observe from these two figures, an increase in the value of e_0a tends to reduce both the frequency and critical mean flow velocity. We conclude that a higher value of e_0a might cause the CNT to lose its stability earlier as compared with the continuum theory predictions where e_0a is set to zero. Moreover, by

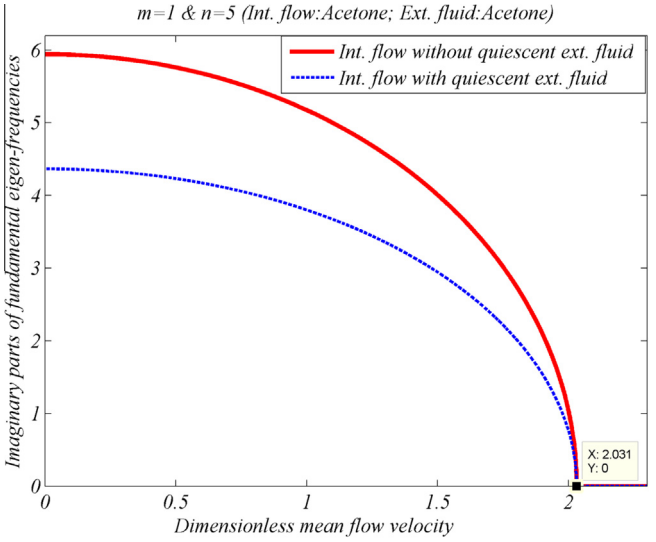

Fig. 8. Imaginary parts of the fundamental eigen-frequencies of simply-supported Donnell's shallow shell conveying an internal flow of acetone with and without a quiescent external fluid of acetone against dimensionless mean flow velocity for an internal fluid of acetone.

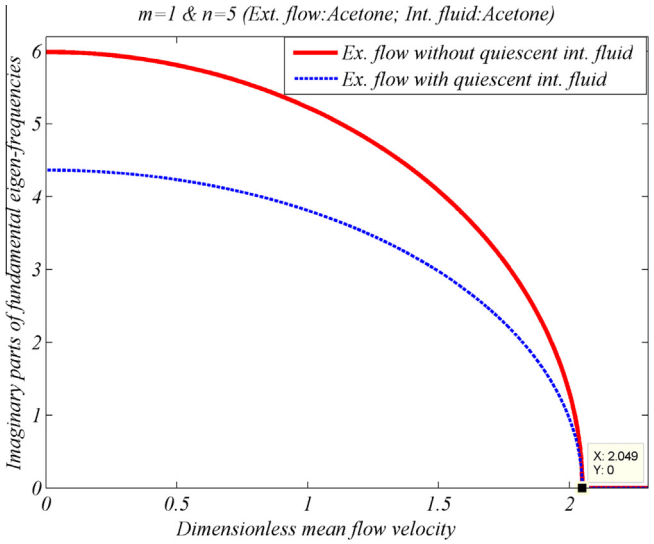

Fig. 9. Imaginary parts of the fundamental eigen-frequencies of simply-supported Donnell's shallow shell conveying an external flow of acetone with and without a quiescent internal fluid of acetone against dimensionless mean flow velocity for an external fluid of acetone.

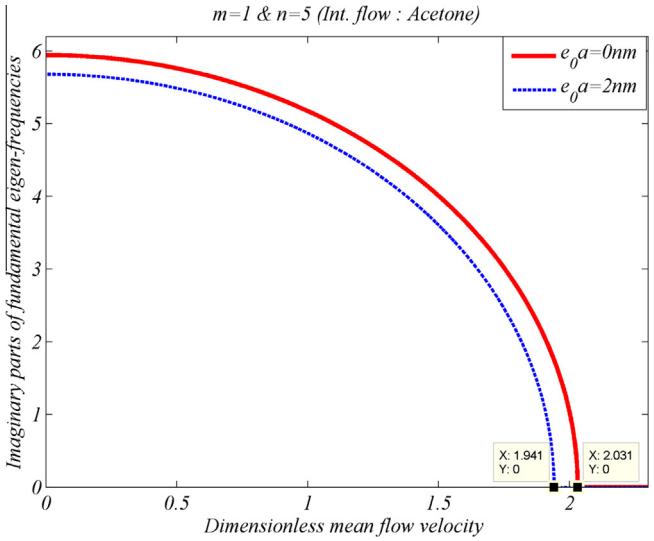

Fig. 10. Imaginary parts of the fundamental eigen-frequencies against dimensionless mean velocity of an internal flow for the simply-supported Donnell's shallow shell CNT conveying a liquid flow, herein acetone, for two different values of nonlocal parameter ($Kn = 0$).

comparing the values of critical mean flow velocities for $e_0a = 2$ nm, we observe approximately a four percent reduction in the magnitude of the critical flow velocity of the first-mode divergence for liquid nano-flow. It is worth mentioning that this percentage of reduction becomes greater for the CNTs with smaller lengths.

4.5. Effect of slip condition on the first-mode divergence

In this section, we deal with the effect of slip boundary condition on the dynamic stability of the nano-shell conveying both internal and external nano-flows by considering classical continuum theory, i.e., $e_0a = 0$ nm. According to Mirramezani and Mirdamadi [35], the range of Kn for a liquid nano-flow, herein acetone, is from zero to 0.001. Fig. 11 portrays the imaginary parts of the vibration eigen-frequencies of a Donnell's shallow shell against the average velocity of the internal liquid flow for two different values of Kn. By comparing the values of critical flow velocities for different Kns, we perceive that Kn could not affect noticeably on the general response of the coupled fluid–structure dynamics. We merely observe that a higher Kn might cause an insignificant positive shift in the divergence happening; in addition, an eigen-frequency of CNT might

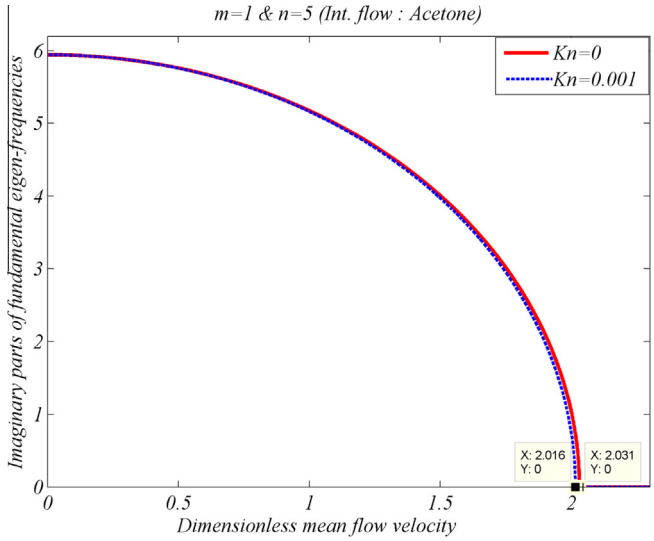

Fig. 11. Imaginary parts of the fundamental eigen-frequencies against dimensionless mean velocity for the simply-supported local Donnell's shallow shell CNT conveying an internal liquid flow, herein acetone, for two different values of *Kn*.

decrease unnoticeably for higher *Kn*s. In contrast, the variation in *Kn* for a gas nano-flow is considered between zero and two, i.e., $0 < Kn < 2$ [35]. Fig. 12 illustrates how the eigen-frequency and the critical mean velocity of the internal gas nano-flow might be affected by different admissible values for *Kn*. The results obtained from Fig. 12 reveal that by increasing *Kn*, the divergence velocity occurs substantially earlier.

For considering the slip boundary condition into the FSI equation of motion, we multiply the undisturbed mean flow velocities, *u*, along the axial direction, by the dimensionless parameter *VCF*. Before going to the details of the influence of slip condition on an external flow, we ought to discuss the concept of VCF_{ef} and compare its value with another close concept, i.e., VCF_{if}. By a thorough investigation of Eqs. (52) and (53), we conclude that VCF_{ef} could depend on the ratio of the R_2 to R_1. Fig. 13 shows VCF_{ef} for different ratios of R_2/R_1 as well as the values of VCF_{if}, against *Kn*. As could be seen, by investigating the value of *Kn* equal to zero, where we have a continuum flow regime with the basic postulate of no-slip condition, the *VCF* for both internal and external flows becomes equal to unity. It means that in the FSI governing equation, the *VCF* should not appear and we reach the conventional well-known FSI equation. Furthermore, we observe that by increasing the ratio of R_2/R_1, the value of *VCF*, devised for an external flow could approach that of *VCF* defined for an internal flow. Figs. 14 and 15 portray the influence of slip condition on the vibrational response of shell-type CNTs conveying external liquid and

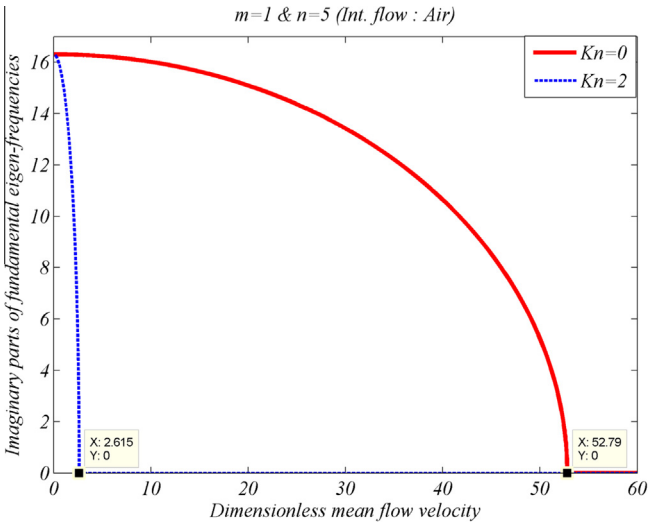

Fig. 12. Imaginary parts of the fundamental eigen-frequencies against dimensionless mean velocity for the simply-supported local Donnell's shallow shell CNT conveying an internal gas flow, herein air, for two different values of *Kn*.

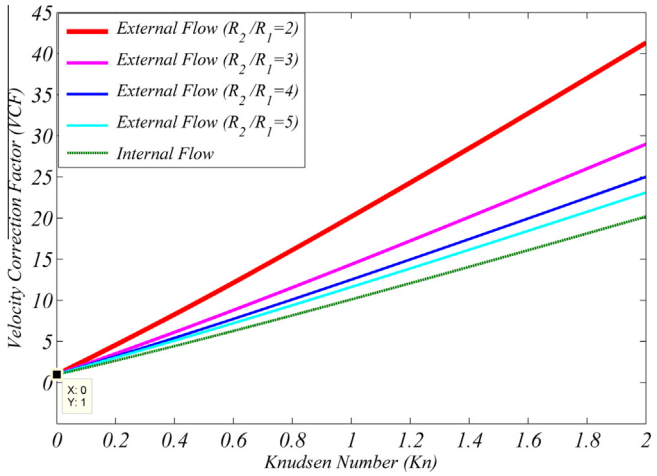

Fig. 13. VCFs for both internal and external flows considering different values of R_2/R_1 against *Kn*.

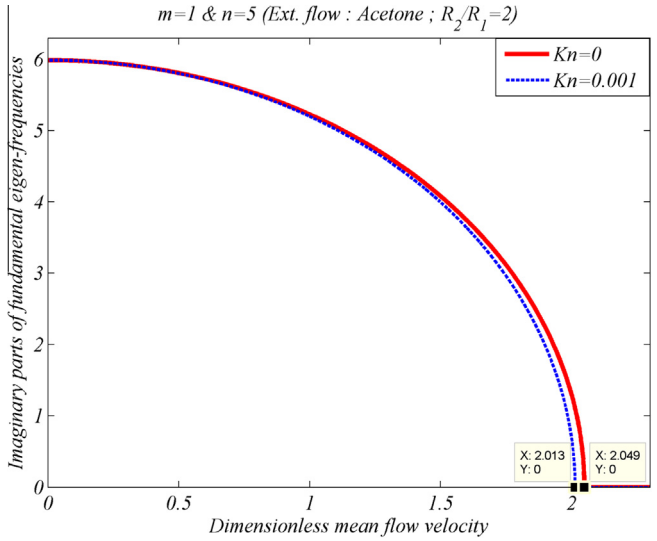

Fig. 14. Imaginary parts of the fundamental eigen-frequencies against dimensionless mean velocity for the simply-supported local Donnell's shallow shell CNT conveying an external liquid flow, herein acetone, for two different values of *Kn*.

gas nano-flows, respectively. The results of these two figures reveal that considering slip boundary condition for an external flow could cause an earlier occurrence for the first-mode divergence instability, as we could observe for an internal flow. It should be mentioned that because VCF_{ef} is greater than VCF_{if}; consequently, *Kn* brings about a more reduction in the critical velocity of an external flow as compared to an internal flow.

4.6. Simultaneous effects of nonlocal parameter and Kn on dynamic stability

In this part, we scrutinize the effect of both nonlocal parameter and *Kn*, simultaneously on the critical flow velocities of CNT conveying internal and external flows, both separately and concurrently. By comparing Fig. 16 with the previous figures, we notice a more reduction in the divergence velocity by taking into account these effects simultaneously, in comparison with the values calculated by considering each effect separately. In addition, as the value of R_2/R_1 increases for the external flows, the critical mean velocity of both internal and external flows, by considering the size effects for both nano-flow and nano-structure becomes very close to each other. Moreover, it is crystal clear that for gas nano-flow, the *Kn* should have greater effects on the earlier occurrence of the first-mode divergence instability of the CNT conveying nano-flow in contrast to the nonlocal parameter. Since we observe approximately more than 95% reduction in the critical velocity by considering both size effects of nano-flow and nano-structure, simultaneously, for CNT conveying gas flow, we conclude that the size effects could play an appreciable role on the stability behavior. Therefore, ignoring the size effects for a gas nano-flow might

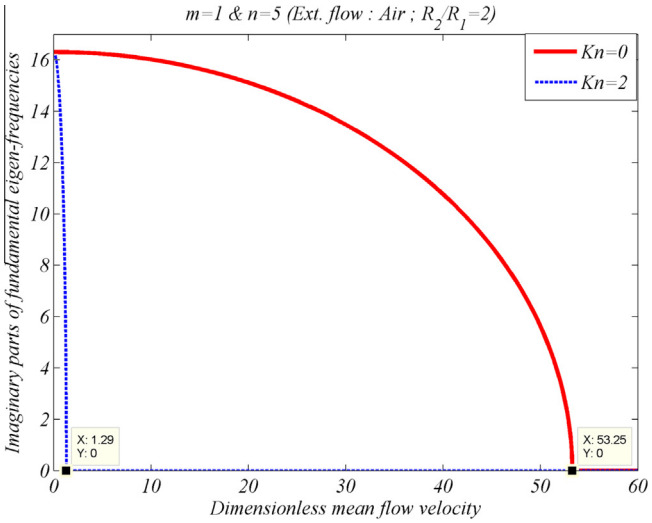

Fig. 15. Imaginary parts of the fundamental eigen-frequencies against dimensionless mean velocity for the simply-supported local Donnell's shallow shell CNT conveying an external gas flow, herein air, for two different values of *Kn*.

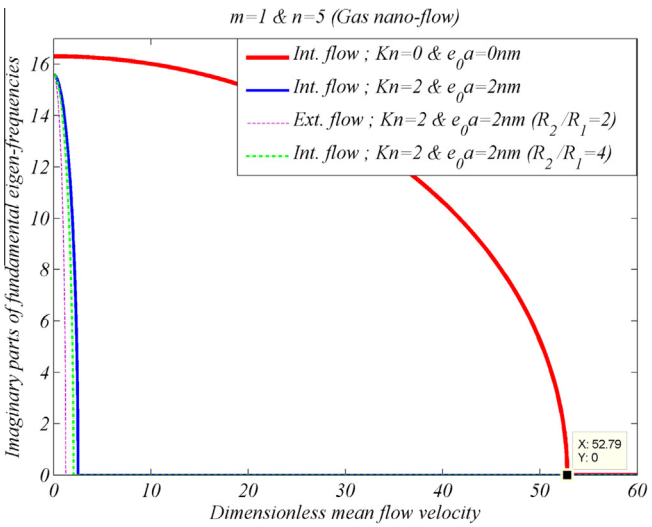

Fig. 16. Imaginary parts of the fundamental eigen-frequencies against dimensionless mean velocity of an internal flow for the simply-supported Donnell's shallow shell CNT conveying both internal and external gas flows, herein air, both accounting for and neglecting the size effects for nano-structure and nano-flow.

cause erroneously a non-conservative structural design of fluidic nano-devices. In the following part, we pay more attention to the size effects of a liquid nano-flow. Fig. 17 demonstrates the imaginary parts of a fundamental eigen-frequency of shell-type CNT against the internal mean flow velocity of acetone. The results obtained from this figure seem to be similar to those observed from Fig. 16; nonetheless, we realize that in a liquid nano-flow, the nonlocal elasticity could have more contribution than *Kn* for a reduction in the critical velocity. With regard to Fig. 17, we observe a greater decline in the value of critical internal velocity by considering a CNT subjected simultaneously to both internal and external flows than the value obtained by analyzing each flow separately. Consequently, the presence of an external flow could impress strikingly the stability response of CNTs conveying an internal flow. Fig. 18 discusses the impression of mass density on the external flow investigating the dynamic behavior of CNTs conveying both internal and external flows by studying a fixed value for the ratio of the external mean flow velocity to the internal mean flow velocity, i.e., u_e/u_i. It is obvious that an increase in the value of mass density of the external flow could result in a greater decrease in the eigen-frequencies as well as the divergence velocity. As a summary, considering the size-effects of both nano-flow and nano-structure as well as the existence of external flow could affect the vibrational behavior of a shell-type CNTs conveying fluid strikingly.

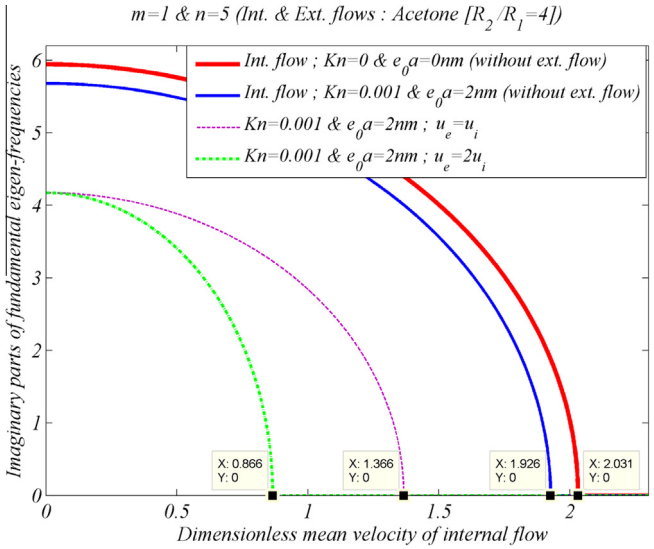

Fig. 17. Imaginary parts of the fundamental eigen-frequencies against mean dimensionless velocity of an internal flow for the simply-supported Donnell's shallow shell CNT conveying both internal and external liquid flows, herein acetone, both accounting for and neglecting the size effects for nano-structure and nano-flow.

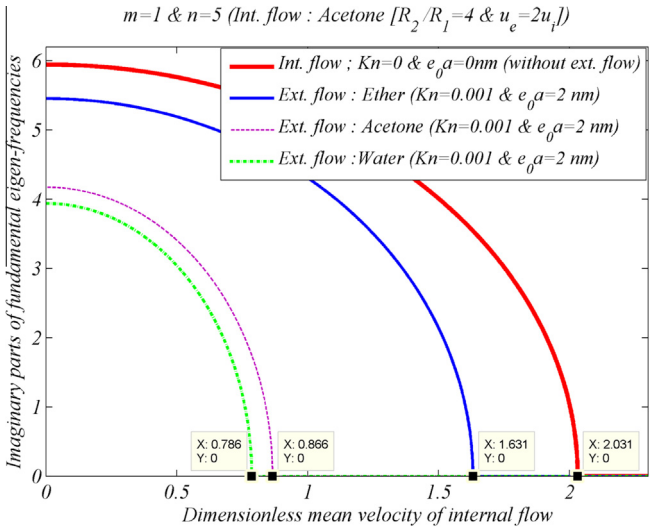

Fig. 18. Imaginary parts of the fundamental eigen-frequencies against dimensionless mean velocity of an internal flow for the simply-supported Donnell's shallow shell CNT conveying an internal acetone flow and three different external flows, herein ether, acetone, and water, both accounting for and neglecting the size effects for nano-structure and nano-flow.

5. Conclusions

This research study addressed the dynamic stability of CNT shell-type structures conveying both internal and external fluid flows and enforcing slip boundary condition between the CNT and passing fluid, as well as implementing Eringen's non-local elasticity theory for the structural part, and Knudsen-dependent flow velocity for nano-flow. For deriving a coupled interaction formulation between the CNT shell structure and passing internal fluid (FSI), the linear Donnell's shallow shell and linear potential flow theory were used. We applied Galerkin's solution of weighted residuals method to transform the BVP of FSI governing equation, including a PDE and the corresponding geometric and natural boundary conditions, into a system of discretized ODEs. We analyzed the effects of both quiescent and moving external fluids on the dynamic behavior of the nano-shell conveying liquid (acetone) and gas (air) internal flows. We observed that the vibration responses of simply-supported Donnell's shell conveying external flow is quite qualitatively similar to that obtained for an internal flow and an insignificant increase in the value of eigen-frequencies and critical velocities of the external flow was observed in contrast to

the internal flow. Moreover, the results revealed that the presence of a quiescent external fluid for shell-type CNT conveying internal flow, could not alter the divergence velocity; nevertheless, the eigen-frequencies of CNT were decreased noticeably due to conceiving a virtual added mass density to the FSI governing equation. In addition, the dynamic response of linear Donnell's shell structure was analyzed by considering each of the nonlocal parameter and slip condition effects separately, and then, by considering both effects simultaneously. We conclude that an increase in the value of nonlocal parameter tends to reduce both the eigen-frequency and critical mean flow velocity. The effect of slip boundary conditions between a CNT and fluid was modeled in FSI problem by devising the dimensionless parameter of *VCF* for the internal as well as the external flow for the first time. We noticed that by increasing the ratio of the outer radius of the inner tube to the inner radius of the outer tube, i.e., R_2/R_1, the value of *VCF* devised for the external flow approaches that of *VCF* defined for an internal flow. We concluded that the effect of slip condition on a liquid nano-flow was not an influential parameter on the nano-flow stability behavior with respect to a continuum flow regime ($Kn = 0$). In contrast, in a gas nano-flow, *Kn* could have remarkable impression on the reduction in the critical mean flow velocity. Then, by analyzing the effects of both *Kn* and nonlocal parameters simultaneously, we perceived a greater amount of decline for the critical flow velocity of the first mode divergence, in contrast to the values calculated by considering each effect separately. Furthermore, the existence of external fluid flow could bring about an appreciable reduction in the eigen-frequency and critical flow velocity of an internal flow. It should be worth mentioning that as the mass density of the external flow becomes greater, we observe an earlier occurrence for the first-mode divergence instability.

Appendix A

$$D_0 = \frac{1}{4\mu}\left(\frac{\partial p}{\partial x}\right)\frac{1}{\left(\ln\frac{R_1}{R_2} - 2\gamma\right)}\left[R_2^2 - R_1^2 + 2\gamma(R_2^2 + R_1^2)\right] \tag{1}$$

$$D_1 = \frac{1}{4\mu}\left(\frac{\partial p}{\partial x}\right)\frac{1}{\left(\ln\frac{R_1}{R_2} - 2\gamma\right)}\left[\begin{array}{l} 2\gamma^2(R_2^2 - R_1^2) + \gamma(R_2^2 + R_1^2) \\ +R_1^2\ln(R_2)(1-2\gamma) - R_2^2\ln(R_1)(1+2\gamma) \end{array}\right] \tag{2}$$

References

[1] G. Hummer, J.C. Rasaiah, J.P. Noworyta, Water conduction through the hydrophobic channel of carbon nanotubes, Nature 414 (2001) 188–190.
[2] Z. Mao, S.B. Sinnott, A computational study of molecular diffusion and dynamics flow through CNTs, J. Chem. Phys. B 104 (2000) 4618–4624.
[3] Y. Gao, Y. Bando, Carbon nano-thermometer containing gallium, Nature 415 (2002) 599.
[4] S. Joseph, N.R. Aluru, Why are carbon nano-tubes fast transporters of water, Nano Lett. 8 (2008) 452–458.
[5] J. Yoon, C.Q. Ru, A. Mioduchowski, Vibration and instability of carbon nano-tubes conveying fluid, Compos. Sci. Technol. 65 (2005) 1326–1336.
[6] T. Natsuki, Q.Q. Ni, M. Endo, Wave propagation in single- and double-walled carbon nanotubes filled with fluids, J. Appl. Phys. 101 (2007) 034319.
[7] W. Lin, N. Qiao, In-plane vibration analysis of curved pipes conveying fluid using the generalized differential quadrature rule, Comput. Struct. 86 (2008) 133–139.
[8] Y. Yan, W.Q. Wang, L.X. Zhang, Noncoaxial vibration of fluid-filled multi-walled carbon nanotubes, Appl. Math. Model. 34 (2010) 122–128.
[9] E. Ghavanloo, F. Daneshmand, M. Rafiei, Vibration and instability analysis of carbon nanotubes conveying fluid and resting on a linear viscoelastic Winkler foundation, Physica E 42 (2010) 2218–2224.
[10] L. Wang, H.L. Dai, Q. Qian, Dynamics of simply supported fluid-conveying pipes with geometric imperfections, J. Fluid Struct. 29 (2012) 97–106.
[11] M.P. Païdoussis, J.P. Denise, Flutter of thin cylindrical shells conveying fluid, J. Sound Vib. 20 (1972) 9–26.
[12] D.S. Weaver, T.E. Unny, On the dynamic stability of fluid-conveying pipes, J. Appl. Mech. 40 (1973) 48–52.
[13] M. Amabili, F. Pellicano, M.P. Païdoussis, Non-linear dynamics and stability of circular cylindrical shells conveying flowing fluid, Comput. Struct. 80 (2002) 899–906.
[14] K.N. Karagiozis, M.P. Païdoussis, M. Amabili, Effect of geometry on the stability of cylindrical clamped shells subjected to internal fluid flow, Comput. Struct. 85 (2007) 645–659.
[15] G.G. Sheng, X. Wang, Thermomechanical vibration analysis of a functionally graded shell with flowing fluid, Eur. J. Mech. A – Solid. 27 (2008) 1075–1087.
[16] M. Amabili, K. Karagiozis, M.P. Païdoussis, Effect of geometric imperfections on non-linear stability of circular cylindrical shells conveying fluid, Int. J. Nonlinear Mech. 44 (2009) 276–289.
[17] R.D. Firouz-Abadi, M.A. Noorian, H. Haddadpour, A fluid–structure interaction model for stability analysis of shells conveying fluid, J. Fluid Struct. 26 (2010) 747–763.
[18] M.J. Hannoyer, M.P. Païdoussis, Instabilities of tubular beams simultaneously subjected to internal and external axial flows, J. Mech. Des. 100 (1978) 328–336.
[19] A. Selmane, A.A. Lakis, Vibration analysis of anisotropic open cylindrical shells subjected to a flowing fluid, J. Fluid Struct. 11 (1997) 111–134.
[20] M. Amabili, F. Pellicano, M.P. Païdoussis, Nonlinear stability of circular cylindrica1 shells in annular and unbounded axial flow, J. Appl. Mech. 68 (2001) 827–834.
[21] J. Koplik, J.R. Banavar, J.F. Willemsen, Molecular dynamics of fluid flow at solid surfaces, Phys. Fluids A 1 (1989) 781–794.
[22] L.A. Pozhar, Structure and dynamics of nanofluids: theory and simulations to calculate viscosity, Phys. Rev. E 61 (2000) 1432–1446.
[23] A. Tounsi, H. Heireche, A. Benzair, I. Mechab, Comment on vibration analysis of fluid-conveying double-walled carbon nanotubes based on nonlocal elastic theory, J. Phys. 21 (2009) 448001.
[24] Y. Zhen, B. Fang, Thermal-mechanical and nonlocal elastic vibration of single-walled carbon nano-tubes conveying fluid, Comput. Mater. Sci. 49 (2010) 276–282.
[25] Y.Z. Wang, F.M. Li, K. Kishimoto, Wave propagation characteristics in fluid-conveying double-walled nanotubes with scale effects, Comput. Mater. Sci. 48 (2010) 413–418.

[26] M. Rafiei, S.R. Mohebpour, F. Daneshmand, Small-scale effect on the vibration of non uniform carbon nanotubes conveying fluid and embedded in viscoelastic medium, Physica E 44 (2012) 1372–1379.
[27] L. Wang, A modified nonlocal beam model for vibration and stability of nanotubes conveying fluid, Physica E 44 (2011) 25–28.
[28] L.L. Ke, Y.S. Wang, Flow-induced vibration and instability of embedded double-walled carbon nanotubes based on a modified couple stress theory, Physica E 43 (2011) 1031–1039.
[29] L. Wang, Vibration analysis of fluid-conveying nanotubes with consideration of surface effects, Physica E 43 (2010) 437–439.
[30] L. Wang, Wave propagation of fluid-conveying single-walled carbon nanotubes via gradient elasticity theory, Comput. Mater. Sci. 49 (2010) 761–766.
[31] T.P. Chang, M.F. Liu, Small scale effect on flow-induced instability of double-walled carbon nanotubes, Eur. J. Mech. A – Solid 30 (2011) 992–998.
[32] H. Jannesari, M.D. Emami, H. Karimpour, Investigating the effect of viscosity and nonlocal effects on the stability of SWCNT conveying flowing fluid using nonlinear shell model, Phys. Lett. A 376 (2012) 1137–1145.
[33] A. Ghorbanpour Arani, M.Sh. Zarei, S. Amir, Z. Khoddami Maraghi, Nonlinear nonlocal vibration of embedded DWCNT conveying fluid using shell model, Physica B 410 (2013) 188–196.
[34] V. Rashidi, H.R. Mirdamadi, E. Shirani, A novel model for vibrations of nano-tubes conveying nano-flow, Comput. Mater. Sci. 51 (2012) 347–352.
[35] M. Mirramezani, H.R. Mirdamadi, The effect of Knudsen-dependent flow velocity on vibration of a nano-pipe conveying fluid, Arch. Appl. Mech. 82 (2012) 879–890.
[36] F. Kaviani, H.R. Mirdamadi, Wave propagation analysis of carbon nano-tube conveying fluid including slip boundary condition and strain inertial gradient theory, Comput. Struct. 116 (2013) 75–87.
[37] M. Mirramezani, H.R. Mirdamadi, Effects of nonlocal elasticity and Knudsen number on fluid–structure interaction in carbon nano-tube conveying fluid, Physica E 44 (2012) 2005–2015.
[38] M.R. Matin, H.R. Mirdamadi, M. Ghayour, Effects of nonlocal elasticity and slip condition on vibration of nano-plate coupled with fluid flow, Physica E 48 (2013) 85–95.
[39] M. Mirramezani, H.R. Mirdamadi, M. Ghayour, Innovative coupled fluid-structure interaction model for carbon nano-tubes conveying fluid by considering the size effects of nano-flow and nano-structure, Comput. Mater. Sci. 77 (2013) 161–171.
[40] L.H. Donnell, Beams, Plates and Shells, McGraw Hill, New York, 1976.
[41] A.C. Eringen, Linear theory of non-local elasticity and dispersion of plane waves, Int. J. Eng. Sci. 10 (1972) 425–435.
[42] A.C. Eringen, On differential equations of nonlocal elasticity and solutions of screw dislocation and surface waves, J. Appl. Phys. 54 (1983) 4703–4710.
[43] M.P. Païdoussis, Fluid–Structure Interactions: Slender Structures and Axial Flow, vol. 2, Elsevier Academic Press, London, 2004.
[44] G. Karniadakis, A. Beskok, N. Aluru, Microflows and Nanoflows: Fundamentals and Simulation, Springer, New York, 2005.
[45] W.G. Pollard, R.D. Present, On gaseous self-diffusion in long capillary tubes, Phys. Rev. 73 (1948) 762–774.
[46] H. Shokouhmand, A.H.M. Isfahani, E. Shirani, Friction and heat transfer coefficient in micro and nano channels filled with porous media for wide range of Knudsen number, Int. Commun. Heat. Mass. 37 (2010) 890–894.
[47] A. Beskok, G.E. Karniadakis, A model for flows in channels, pipes, and ducts at micro and nano scales, Microscale Therm. Eng. 3 (1999) 43–77.
[48] F.M. White, Fluid Mechanics, McGraw-Hill, New York, 1982.
[49] M.P. Païdoussis, Fluid–Structure Interactions: Slender Structures and Axial Flow, vol. 1, Academic Press, London, 1998.
[50] M. Amabili, Nonlinear Vibrations and Stability of Shells and Plates, Cambridge University Press, New York, 2008.
[51] C.Q. Ru, Effective bending stiffness of carbon nanotubes, Phys. Rev. B 62 (2000) 9973–9976.
[52] Q. Wang, V.K. Varadan, S.T. Quek, Small scale effect on elastic buckling of carbon nanotubes with nonlocal continuum models, Phys. Lett. A 357 (2006) 130–135.